(correlation factor $R = 0.99$) and 6.1 kJ/(mol·K) ($R = 0.86$) for GeBr$_4$, and 6.8 ($R = 0.98$) and 7.0 kJ/(mol·K) ($R = 0.94$) for GeI$_4$, respectively. These values may be regarded as essentially identical within experimental errors and are reasonable compared with 7.6 kJ/(mol·K) for CCl$_4$[10] and 9.2 kJ/(mol·K) for Sn(CH$_3$)$_4$.[11] These results give a confirmative evidence that the scalar coupling relaxation is involved in the relaxation of ^{73}Ge in GeBr$_4$ and GeI$_4$.

Germanium–Halogen Coupling Constants. As described in our previous paper,[6] eq 5 for the two isotopes of Br, i.e., ^{79}Br and ^{81}Br, are converted to eq 6 and 7, where, τ_1^{81} and τ_1^{127} are T_1 of ^{81}Br

GeBr$_4$: $(T_2^{sc})^{-1} = 4.04 A_{81}{}^2 \tau_1^{81}$ (6)

GeI$_4$: $(T_2^{sc})^{-1} = 11.7 A_{127}{}^2 \tau_1^{127}$ (7)

and ^{127}I in GeBr$_4$ and GeI$_4$, respectively. However, no experimental results of τ_1 have been reported due to extremely broad signals for Br and I.

Johnson et al.[12] reported that T_2 values for ^{35}Cl in GeCl$_4$ and SnCl$_4$ were 4.1×10^{-5} and 2.2×10^{-5} s, respectively, while Sharp[13]

(10) Lassigne, C. R.; Wells, E. J. *J. Magn. Reson.* 1977, *26*, 55.
(11) Gillen, K. T.; Noggle, J. H.; Leipert, T. K. *Chem. Phys. Lett.* 1972, *17*, 505.
(12) Johnson, K. J.; Hunt, J. P.; Dodgen, H. W. *J. Chem. Phys.* 1969, *51*, 4493.
(13) Sharp, R. R. *J. Chem. Phys.* 1974, *60*, 1149.

reported that T_1 values for ^{81}Br and ^{127}I in SnBr$_4$ and SnI$_4$ were 7.5×10^{-7} (21 °C) and 1.5×10^{-7} s (150 °C), respectively. If the ratio $T_2(^{35}$Cl$)$ of GeCl$_4$/$T_{1,2}(^{35}$Cl$)$ of SnCl$_4$ is equal to $T_2(^{81}$Br$)$ of GeBr$_4$/$T_{1,2}(^{81}$Br$)$ of SnBr$_4$ or $T_2(^{127}$I$)$ of GeI$_4$/$T_{1,2}(^{127}$I$)$ of SnI$_4$, $T_2(^{81}$Br$)$ of GeBr$_4$ and $T_2(^{127}$I$)$ of GeI$_4$ will be 1.4×10^{-6} and 2.8×10^{-7} s, respectively. That is, we are using an analogy with X in SnX$_4$ to estimate $T_{1,2}(X)$ in GeX$_4$, and we found that $T_{1,2}$ becomes shorter in the order Cl → Br → I. Though there is no theoretical justification for this assumption, the similarity of the relaxation mechanism among these nuclei seem to allow our treatment at least in a semiquantitative manner. By substituting these values for τ_1 in eq 6 and 7, we estimate the coupling constants of J(Ge–Br) and J(Ge–I) as 64 and 220 Hz, respectively.

The contribution of scalar coupling relaxation to the relaxation mechanism decreases in the order GeCl$_4$ → GeBr$_4$ → GeI$_4$; i.e., the scalar coupling mechanism appears at high temperature in that order. This is because T_1 becomes shorter in the order Cl → Br → I.

In conclusion, the contribution of scalar coupling in the spin-spin relaxation of ^{73}Ge in all halogermanes is now established. The extent of this contribution is, however, a function of temperature, and hence at room temperature this is observed only for GeCl$_4$ and GeBr$_4$.

Registry No. GeBr$_4$, 13450-92-5; GeI$_4$, 13450-95-8; ^{73}Ge, 15034-58-9.

Contribution from the Institut für Anorganische Chemie, Universität Bern, CH-3000 Bern 9, Switzerland, Institut für Anorganische Chemie, Universität Mainz, D-6500 Mainz, West Germany, Laboratorium für Kristallographie, Universität Bern, CH-3012 Bern, Switzerland, and Physik Department, Technische Universität München, D-8046 Garching, West Germany

Mössbauer Spectra and Electronic Ground-State Calculations of Strongly Coupled Ruthenium Ammines Bridged by Pyrazine and *p*-Benzoquinone Diimine

Stefan Joss,[1a] Kai M. Hasselbach,[1b] Hans-Beat Bürgi,*,[1c] Rainer Wordel,[1d] Friedrich E. Wagner,[1d] and Andreas Ludi*,[1a]

Received May 26, 1988

The electronic structure of the ligand-bridged binuclear ions [(NH$_3$)$_5$Ru–pyz–Ru(NH$_3$)$_5$]$^{n+}$ ($n = 4$–6; pyz = pyrazine) and [(NH$_3$)$_5$Ru–bqd–Ru(NH$_3$)$_5$]$^{m+}$ ($m = 4$, 5; bqd = benzoquinone diimine) is discussed in terms of a self-consistent-charge extended Hückel (SCCEHMO) approach. One-electron molecular orbitals are obtained by using valence-state ionization potentials for all of the atoms. Configurational energies are adjusted to the experimentally determined g values. The resulting wave functions were used to calculate isomer shifts and quadrupole splittings for the ^{99}Ru Mössbauer spectra of the various ruthenium dimers. Observed isomer shifts for the two mixed-valence ions are −0.535 (pyz) and −0.507 mm s^{-1} (bqd), and quadrupole splittings are 0.513 and 0.571 mm s^{-1}, respectively. The generally good agreement between calculated and observed quantities in conjunction with results deduced from the molecular structures is fully compatible with a symmetric structure for the two mixed-valence ions.

Introduction

Discussion of the electronic structure of ligand-bridged binuclear mixed-valence compounds continues to deal with the question whether a given compound [M–L–M]$^{\mu+\nu}$ is best described as localized, [M$^{\mu+}$–L–M$^{\nu+}$] (class II), or delocalized [M$^{(\mu+\nu)/2}$–L–M$^{(\mu+\nu)/2}$] (class III).[2] This classification scheme, as well as the approach by Hush,[3] has evolved from theoretical treatments of outer-sphere electron-transfer reactions. Neither these approaches nor the vibronic coupling model developed by Schatz[4] consider the electronic structure of the bridging ligand L explicitly. This may not present problems for the description of the weakly coupled metal ions typical for outer-sphere electron-transfer reactions, but it is a shortcoming for cases with strong metal–metal coupling mediated by bridging ligands.

The most prominent example of a stable mixed-valence dimer is the Creutz–Taube ion,[5] [(NH$_3$)$_5$Ru–pyz–Ru(NH$_3$)$_5$]$^{5+}$, abbreviated as [II-pyz-III].[6] Most experimental results for this compound may be explained in terms of a delocalized description, e.g. the crystallographic results for the complete electron-transfer series.[7] Taken together with structural data for [II-bqd-III],[8] they show a significant dependence of the Ru–N(bridge) distance on the oxidation state and on the electronic properties of the bridge.

(1) (a) Institut für Anorganische Chemie, Universität Bern. (b) Universität Mainz. Present address: Dr. K. Thomae GmbH, Biberach, West Germany. (c) Laboratorium für Kristallographie, Universität Bern. (d) Technische Universität München.
(2) Robin, M. B.; Day, P. *Adv. Inorg. Chem. Radiochem.* 1967, *10*, 247.
(3) Hush, N. S. *Prog. Inorg. Chem.* 1967, *8*, 391.
(4) Wong, K. Y.; Schatz, P. N. *Prog. Inorg. Chem.* 1981, *28*, 370.
(5) (a) Creutz, C.; Taube, H. *J. Am. Chem. Soc.* 1969, *91*, 3988; 1973, *95*, 1086. (b) Creutz, C. *Prog. Inorg. Chem.* 1983, *30*, 1.
(6) Throughout this paper the self-explanatory abbreviations [II-pyz-II], [II-pyz-III], [III-pyz-III], [II-bqd-II], and [II-bqd-III] will be used without implying well-defined oxidation states; pyz is pyrazine

bqd is *p*-benzoquinone diimine
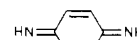
(7) Fürholz, U.; Joss, S.; Bürgi, H.-B.; Ludi, A. *Inorg. Chem.* 1985, *24*, 943.
(8) Joss, S.; Bürgi, H.-B.; Ludi, A. *Inorg. Chem.* 1985, *24*, 949.

Table I. Important Molecular Orbitals for [II-pyz-III] and [II-bqd-III]

[II-pyz-III]

| | main parent orbitals | | | $-E$, eV | ΔE, cm^{-1} | % contribn | | |
	Ru 4d	N 2p(pyz)	C 2p			Ru 4d	N 2p(pyz)	C 2p
$14b_g(\pi_6)$	xz	x	x	4.43	66 540	0.7	26.9	70.7
$20a_g$	z^2	z	z	7.07	45 250	51.7	12.9	0.5
$20b_u$	z^2	z	z	7.31	43 310	54.0	11.7	0.6
$14a_u$	xy		x	7.65	40 570	43.9		19.4
$13b_g$	xy			7.70	40 170	54.8		
$13a_u(\pi_5)$	xy		x	7.89	38 640	11.0		79.3
$12a_u(\pi_4) = \phi_7$	xz	x	x	9.96	21 940	9.4	62.1	27.5
$12b_g = \phi_6$	xz	x	x	12.68	0	89.4	3.9	4.5
$19a_g = \phi_5$	yz	y	y, z	12.76	650	94.1	1.3	1.5
$19b_u = \phi_4$	yz	y	z, y	12.78	810	95.5	0.6	1.4
$18a_g = \phi_3$	$x^2 - y^2$	z	z	12.85	1 370	96.3	0.1	0.1
$18b_u = \phi_2$	$x^2 - y^2$			12.85	1 370	96.5		
$11a_u = \phi_1$	xz	x	x	13.11	3 470	86.8	4.0	6.5
$17a_g$	z^2	x	x	14.10	11 450	4.1	37.9	24.5
$11b_g(\pi_3)$			x	14.85	17 500			98.8
VOIP Ru 4d				13.102				

[II-bqd-III]

| | main parent orbitals | | | $-E$, eV | ΔE, cm^{-1} | % contribn | | |
	Ru 4d	N 2p(bqd)	C 2p			Ru 4d	N 2p(bqd)	C 2p
$15b_g(\pi_8)$	xz	x	x	2.11	80 900	0.1	4.7	94.3
$15a_u(\pi_7)$	xz	x	x	6.60	44 690	1.0	19.6	79.0
$22a_g$	z^2	z	z, y	6.89	42 350	52.4	11.8	0.6
$22b_u$	z^2	z	y, z	6.92	42 100	52.5	11.8	0.6
$14a_u(\pi_6)$	xy		x	7.15	40 250	1.2		97.0
$14b_g$	xy			7.64	36 300	54.9		
$13a_u$	xy		x	7.65	36 220	53.8		1.8
$13b_g(\pi_5) = \phi_7$	xz	x	x	10.82	10 650	19.5	49.0	30.2
$12a_u = \phi_6$	xz	x	x	12.14	0	64.2	21.2	12.7
$21a_g = \phi_5$	yz	y	y, z	12.64	4 030	94.3	0.7	1.1
$21b_u = \phi_4$	yz	y	y, z	12.65	4 110	94.8	0.6	0.8
$20a_g = \phi_3$	$x^2 - y^2$		z	12.76	5 000	96.4		0.1
$20b_u = \phi_2$	$x^2 - y^2$			12.76	5 000	96.5		
$12b_g = \phi_1$	xz	x	x	13.10	7 740	74.6	4.4	18.7
$11b_g(\pi_3)$	xz		x	13.76	13 070	0.5		98.5
$19a_g$	z^2	z	z	13.98	14 840	2.1	19.1	46.5
$11a_u(\pi_4)$	xz	x	x	14.06	15 490	32.0	42.3	19.4
VOIP Ru 4d				13.020				

Some of the available physical data for [II-pyz-III] can be rationalized not only by the delocalized model but also in terms of a localized d^6–d^5 description. Examples are single-crystal EPR spectra,[9] the effect of a one-electron reduction on the visible absorption band,[5] and the near coincidence of infrared and Raman frequencies.[10]

In this contribution new experimental Mössbauer data for [II-bqd-II] and [II-bqd-III] are reported. These and earlier results are compared to isomer shifts and quadrupole splittings calculated from a self-consistent-charge extended Hückel approach (SCCEHMO) adjusted to reproduce experimental g values. Symmetric structures (Figure 1) of the bqd- and pyz-bridged dimers[7,8] as obtained from X-ray diffraction are used for the calculations. RuO_4 and the two hexaammines $Ru(NH_3)_6^{2+}$ and $Ru(NH_3)_6^{3+}$ are included in the calculations as points of reference. The theoretical approach to reproduce and predict Mössbauer data explicitly takes the electronic structure of the bridging ligand into account. A recently published study of the Creutz–Taube ion also includes the electronic structure of the bridging pyrazine but uses a different theoretical model.[11]

Experimental Section

Preparation of the compounds, their molecular structures,[7,8] and measurements of single-crystal and powder EPR spectra[9] are described

elsewhere. ^{99}Ru Mössbauer spectra of [II-bqd-II] and [II-bqd-III] were recorded with a ^{99}Rh source produced by the (d, 3n) reaction in metallic, isotopically enriched ^{100}Ru; source and absorber were both at liquid-He temperature.

Model Calculations

Nonrelativistic quantum-chemical calculations were performed in four steps: (i) One-electron molecular orbitals ϕ_i were generated by using the SCCEHMO approach (Table I).[12a] (ii) Symmetry-adapted configurational functions $\Theta_i(S, M_s, \Gamma, M_\Gamma)$ were constructed. (iii) The many-electron state function ψ_k, including spin–orbit coupling,[12b] was calculated. This step has been parametrized to reproduce observed g values. Specifically, the energy differences between the ground configuration and the two lowest excited configurations of the same parity have been adjusted.[13] For [II-pyz-III], $E(\Theta_3) - E(\Theta_6) = 1800$ cm^{-1} and $E(\Theta_5) - E(\Theta_6)$

(9) Stebler, A.; Ammeter, J. H.; Fürholz, U.; Ludi, A. *Inorg. Chem.* **1984**, *23*, 2764.

(10) Fürholz, U.; Bürgi, H.-B.; Wagner, F. E.; Stebler, A.; Ammeter, J. H.; Krausz, E.; Clark, R. J. H.; Stead, M. J.; Ludi, A. *J. Am. Chem. Soc.* **1984**, *106*, 121.

(11) Zhang, L.-T.; Ko, J.; Ondrechen, M. J. *J. Am. Chem. Soc.* **1987**, *109*, 1666, 1672.

(12) (a) McGlynn, S. P.; Vanquickenborne, L. G.; Kinoshita, M.; Carroll, D. G. *Introduction to Applied Quantum Chemistry*; Holt, Reinhart, and Winston: New York, 1972. (b) ζ_0 and ζ_1 values (cm^{-1}) were taken as 1000 and 50 (Ru), 78 and 20 (N), 32 and 10 (C): Griffith, J. S. *Theory of Transition Elements*; University Press: Cambridge, 1971. Fraga, S.; Karowski, J.; Saxena, K. M. S. *Handbook of Atomic Data*; Elsevier: Amsterdam, 1976.

(13) For [II-pyz-III] the state energies required to reproduce the observed g tensor are 0, 2040, and 3075 cm^{-1}, in fair agreement with values obtained by Dubicki et al.[14] (0, 2171, and 3201 cm^{-1}), who used an effective Hamiltonian method. Although this extended Hückel model satisfactorily describes ground-state properties, it cannot reproduce optical transition energies in a similar way. Different theoretical approaches[11,15] or additional assumptions[24] are required.

(14) Dubicki, L.; Ferguson, J.; Krausz, E. R. *J. Am. Chem. Soc.* **1985**, *107*, 179.

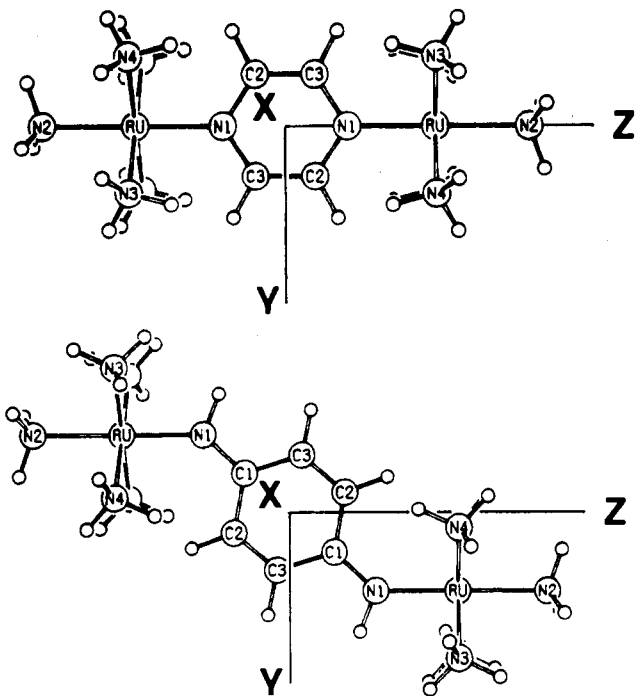(15) Krausz, E. R.; Mau, A. W. H. *Inorg. Chem.* **1986**, *25*, 1484.

Figure 1. Geometry and numbering scheme for ruthenium dimers bridged by pyrazine (top) and *p*-benzoquinone diimine (bottom).

Figure 2. ^{99}Ru Mössbauer spectra of [II-bqd-II] and [II-bqd-III].

= 2600 cm^{-1}; for [II-bqd-III], $E(\Theta_4) - E(\Theta_6)$ = 2000 cm^{-1} and $E(\Theta_2) - E(\Theta_6)$ = 3000 cm^{-1}. Observed[9] (calculated) *g* values for [II-pyz-III] are g_x = 1.346 (1.346), g_y = 2.799 (2.787), g_z = 2.487 (2.404). (iv) Expectation values for a selection of observables were computed. The elements of the **g** tensor are calculated by using the operator $-\beta \mathbf{H}(\hat{\mathbf{L}} + 2\hat{\mathbf{S}})$. Details of the calculations are given elsewhere.[16]

Isomer shifts of the ^{99}Ru Mössbauer spectra were calculated according to eq 1. δ is a function of the electron density at the

$$\delta = (2\pi/3)Ze^2(\langle r_e^2 \rangle - \langle r_g^2 \rangle)(\rho(0)_A - \rho(0)_S) \quad (1)$$

nucleus, $\rho(0)$, and of the nuclear radii *r* in the nuclear ground (g) and excited state (e), where the subscripts A and S refer to absorber and source of the γ-radiation.

$\rho(0)$ is not directly obtained from the SCCEHMO procedure. It has been calculated by Schmidt orthogonalization of the valence orbitals to the core orbitals.[17] $\rho(0)$ consists of several contributions, diagonal terms from the core (c) and the valence (v) orbitals, respectively, as well as overlap contributions between the two: c–c, v–v, and c–v.[18] All these terms are included in our calculations.[16]

Quadrupole splittings were calculated according to eq 2.

$$\Delta = \tfrac{1}{2}eQ_e(1 - R_0)V_{yy}(1 + \eta^2/3)^{1/2}$$
$$\eta = |(V_{xx} - V_{zz})|/V_{yy} \quad (2)$$

The electric field gradient (efg) tensor **V** contains two contributions: one from the Ru valence shell and one from the environment of Ru (lattice). The latter contribution is calculated to be very small and is subsequently neglected. The expectation values $\langle V_{ij} \rangle$ (*i*, *j* = *x*, *y*, *z*) are broken up into sums of matrix elements of the one-electron operator $V_{ij} = [1 - \gamma(r)]Ze(3ij - r^2\delta_{ij})/r^5$.[18] The calculation of the elements V_{ij} of the efg tensor involves the evaluation of one-, two-, and three-center integrals.[19] The radial dependence of the Sternheimer factor $\gamma(r)$[18] is approximated by a superposition of two Gaussians;[20] its asymptotic
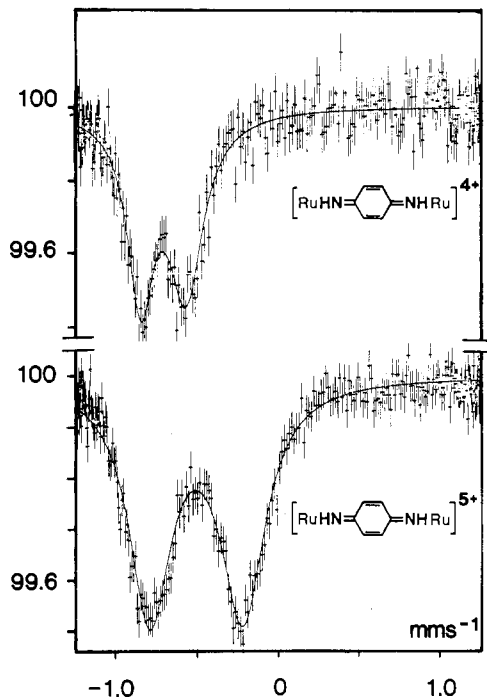
value γ^∞ is –20. In the general expression for the quadrupole splitting (eq 2) with $|V_{yy}| > |V_{xx}| > |V_{zz}|$,[21] the quadrupole moment Q_e of ^{99}Ru was taken as 0.34 b, and the shielding factor[22] $(1 - R_0)$ as 0.68.

SCCEHMO and open-shell calculations were performed on the Honeywell-Bull computer of the University of Mainz by using the local quantum-chemical program system.[16]

Results and Discussion

The spectra for [II-pyz-II], [II-pyz-III], [III-pyz-III], and [Ru^{II}–pyz–Rh^{III}] have been published in ref 10. All four compounds clearly show quadrupole-split doublets. Earlier Mössbauer spectra of the Creutz–Taube ion were interpreted in terms of a superposition of signals, a broad singlet corresponding to Ru(II) and a doublet corresponding to Ru(III) (class II).[23] Our studies with considerably improved statistical accuracy no longer support this. The spectrum of the Creutz–Taube ion shows *one* quadrupole split doublet[10] with an isomer shift that is not midway between those of the [II,II] and [III,III] ions. Analogously, the spectra of [II-bqd-II] and [II-bqd-III] each show a single doublet (Figure 2). The magnitude of δ (referred to Ru metal) serves as a diagnostic label for a given compound and as a rough indicator of the oxidation state of ruthenium.[18]

The isomer shifts δ were compared to the charge q(Ru) obtained from simple HMO calculations for the [II,II] and [II,III] ions.[8] With the assumption that the populations of all but the 4d$_{xz}$(Ru) atomic orbitals are very similar within a series of compounds, q(Ru) is determined by the population number b_{xz} for the *xz* orbital, the metal orbital capable of overlap with the π-system of the ligand bridge. We find an empirical correlation between δ and b_{xz} (Figure 3), indicating that the Ru-bridge π-interaction affects δ, presumably by modifying the charge on Ru. Conversely, δ may be used as a measure of relative charge within a series of compounds.

In addition SCCEHMO calculations were performed for the ligand-bridged dimers, the two hexaammineruthenium ions and RuO$_4$. Test calculations on [III-pyz-III] showed that spin–orbit

(16) Hasselbach, K. M. "Quantum Chemical Program System"; Computer Center, University of Mainz, West Germany.
(17) Clementi, E.; Roetti, C. *At. Data Nucl. Data Tables* **1974**, 14.
(18) Gütlich, P.; Link, R.; Trautwein, A. *Mössbauer Spectroscopy and Transition Metal Chemistry*; Springer: Berlin, Heidelberg, New York, 1978.
(19) Rüdenberg, K. *J. Chim. Phys.* **1951**, *19*, 1433.

(20) Grodzicki, M. Personal communication.
(21) Because the largest component of the efg coincides with the *y* axis of the molecular coordinates, we have interchanged *z* and *y* with respect to the conventional setting of ref 18.
(22) Guenzberger, D.; Garnier, A.; Danon, J. *Inorg. Chim. Acta* **1977**, *21*, 119.
(23) Creutz, C.; Good, M. L.; Chandra, S. *Inorg. Nucl. Chem. Lett.* **1973**, *9*, 171.

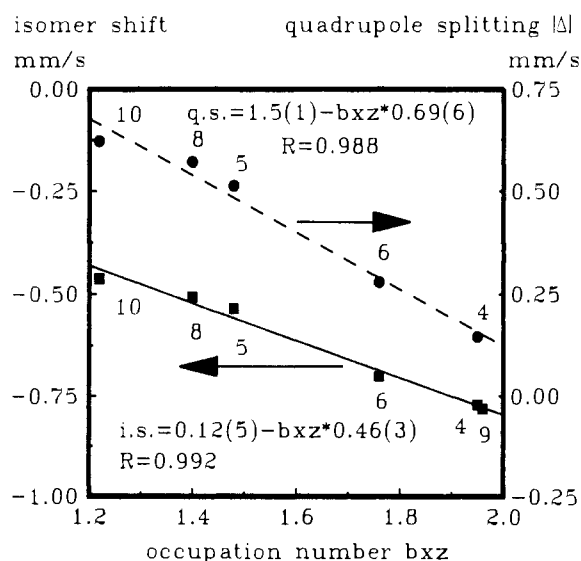**Table II.** Comparison of Observed and Calculated Isomer Shifts

	δ_{obs}, mm s^{-1}	δ_{calc},[a] mm s^{-1}	$\rho(0)$[b]	D_{c-c}	D_{v-v}	O_{c-c}	O_{v-v}	O_{c-v}
RuO$_4$	1.06[c]	1.06	109 535.0	109 492.0	4.0	8.7	0.10	30.2
Ru(NH$_3$)$_6$$^{3+}$	-0.49[c]	-0.39	109 491.1	109 465.2	3.3	4.2	0.04	18.3
Ru(NH$_3$)$_6$$^{2+}$	-0.91[d]	-0.87	109 476.7	109 459.1	2.2	2.7	0.03	12.7
[II-pyz-II]	-0.772[e]	-0.78	109 479.3	109 460.9	2.3	2.6	0.03	13.4
[II-pyz-III]	-0.535[e]	-0.58	109 485.4	109 463.6	2.7	3.3	0.04	15.8
[III-pyz-III]	-0.454[e]	-0.41	109 490.6	109 465.1	3.2	4.2	0.04	18.1
[II-bqd-II]	-0.701[f]	-0.70	109 481.8	109 462.7	2.4	2.6	0.04	14.1
[II-bqd-III]	-0.507[f]	-0.58	109 485.4	109 464.0	2.7	3.1	0.04	15.7

[a] Calculated according to $\delta_{calc} = 0.033(\rho(0) - 109503)$. [b] $\rho(0) = D_{c-c} + D_{v-v} + O_{c-c} + O_{v-v} + O_{c-v}$; D = diagonal, O = overlap, c = core, v = valence contribution; all terms in e/au^3; cf. ref 16 and 18. [c] Kaindl, G.; Wagner, F.; Zahn, U.; Mössbauer, R. C. *Z. Physik* **1969**, *226*, 103. [d] Prados, R.; Clausen, C.; Good, M. L. *J. Coord. Chem.* **1973**, *2*, 201. [e] Reference 10. [f] This work.

Table III. ^{99}Ru Mössbauer Spectra: Observed Quadrupole Splittings Δ and Half-Widths W (mm s^{-1}) and Calculated Parameters
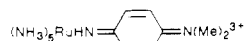
	exptl			calc		
	$|\Delta|$	$W1$	$W2$	Δ	V_{yy}	η
[II-pyz-II][a]	0.146 (7)	0.20 (1)	0.20 (2)	-0.148	-0.263	0.27
[II-pyz-III][a]	0.513 (4)	0.28 (1)	0.36 (1)	-0.560	-1.011	0.02
[III-pyz-III][a]	0.376 (3)	0.24 (1)	0.24 (1)	+0.553	+0.994[c]	0.12
[II-bqd-II][b]	0.280 (10)	0.26 (2)	0.20 (2)	-0.252	-0.449	0.25
[II-bqd-III][b]	0.571 (9)	0.34 (2)	0.31 (2)	-0.577	-1.041	0.04

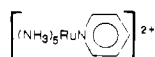[a] Reference 10. [b] This work. [c] Largest component in z direction ($=V_{zz}$).

Figure 3. Correlation of HMO parameters with Mössbauer data (see caption for Figure 4).

Figure 4. Correlation of Mössbauer isomer shifts with electron densities obtained from SCCEHMO calculations: (1) RuO$_4$; (2) Ru(NH$_3$)$_6$$^{3+}$; (3) Ru(NH$_3$)$_6$$^{2+}$; (4) [II-pyz-II]; (5) [II-pyz-III]; (6) [III-pyz-III]; (7) [II-bqd-II]; (8) [II-bqd-III]; (9) [II-py];[25] (10) [II-bqd(Me)$_2$].[25]

coupling does not affect $\rho(0)$ significantly. Therefore, values of $\rho(0)$ were calculated with MO configurations unperturbed by applying spin–orbit corrections. The results presented in Table II show that $\rho(0)$ is dominated by the diagonal core contributions. The variations of the other contributions are of magnitude similar to those of the core contributions and show roughly the same trend. It has to be emphasized that the mutual dependence of the various contributions to $\rho(0)$ is highly complex.[16,24] We may point out that the results for the two bqd complexes given in Tables II and III have been computed prior to the corresponding experimental measurements. The good agreement between experimental and calculated values justifies the choice of the theoretical model.
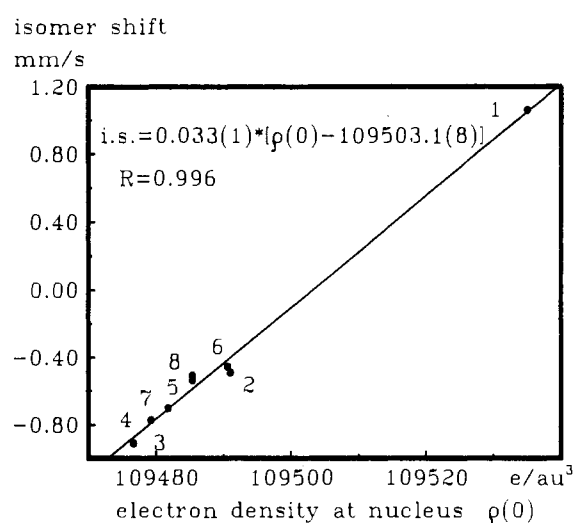
(24) Hasselbach, K. M. To be submitted for publication.
(25) Experimental Mössbauer data (mm s^{-1}) for mononuclear

$(NH_3)_5RuHN$⟨benzene ring⟩$=N(Me)_2$$^{3+}$

are δ = 0.463 (10), $|\Delta|$ = 0.622 (10), $W1$ = 0.321 (21), and $W2$ = 0.320 (17) and for [II-py] =

$[(NH_3)_5RuN$⟨pyridine ring⟩$]$$^{2+}$

δ = -0.782 (3) and W = 0.267 (9).

Again, a reasonable empirical correlation between δ and $\rho(0)$ is observed (Figure 4).

For noncubic site symmetries the nuclear quadrupole moment of ^{99}Ru and the electric field gradient (efg) at the nucleus interact to produce a splitting of the nuclear states with spins $I_g = ^5/_2$ and $I_e = ^3/_2$. The quadrupole splitting for the ground state is significantly smaller than that for the excited state and cannot be resolved unless the efg is very large. Usually one observes a symmetric quadrupole doublet corresponding to the splitting Δ of the excited state. Its two components consist of three unresolved lines, reflecting the splitting of the ground state.

With some simple assumptions the observed values for $|\Delta|$ can be related to the occupation numbers b_{xz} obtained from HMO calculations (Figure 3): If the population numbers are equal among the antibonding 4d$_{xy}$ and 4d$_{z^2}$, as well as the 5p orbitals, these shells do not contribute to the efg owing to their spherical symmetry. If furthermore the nonbonding 4d$_{yz}$ and 4d$_{x^2-y^2}$ orbitals are doubly occupied, the components V_{ii} of the efg tensor can be calculated readily,[18] and a simple linear dependence on b_{xz} is obtained.

$$V_{yy} = -2V_{xx} = -2V_{zz} = 7(e\langle r^{-3}\rangle)^{-1}(b_{xz} - 2)$$

Within this approximation the principal axes of the calculated

efg tensor exactly coincide with the molecular coordinate system of Figure 1. In the more detailed SCCEHMO calculations they almost coincide.

The absolute values of calculated quadrupole splittings for the [II,II] and [II,III] ions are in very good agreement with the observed data (Table III). We notice that the largest efg component is still V_{yy}, i.e. the component within the pyrazine plane perpendicular to the Ru–N(bridge) direction. The sign of the efg cannot be determined from powder spectra unless the triplet structure of the two components of the spectrum is resolved or, at least, manifests itself in visible asymmetries of the pattern. Such asymmetries begin to become noticeable when the splitting Δ of the excited state exceeds about 0.5 mm s^{-1}. For [II,II] it is impossible to even guess the sign, while the [II,III] and [III,III] species are just at the limit where the sign of V_{yy} should become detectable. Owing to additional complications such as axially nonsymmetric efg tensors, unknown preferred orientation of the crystallites in the sample, and anisotropies of the Debye–Waller factor, we have to refrain from drawing any conclusions about the sign of V_{yy} from the experimental data.

The time scale of ^{99}Ru Mössbauer spectroscopy is about 10^{-8} s. For a mixed-valence compound in which the valences are trapped for times longer than about 10^{-8} s, the spectrum should show two separate doublets with different isomer shifts δ and quadrupole splittings Δ corresponding to genuine Ru(II) and Ru(III) moieties, specifically $\Delta(\text{Ru(III)}) > \Delta(\text{Ru(II)})$. For a mixed-valence compound with valences trapped during less than 10^{-8} s, coalescence to one doublet is expected. We interpret our experimental result as strong evidence that on the Mössbauer time

scale the Creutz–Taube ion cannot be described as a localized, class II system and that there exists a strong interaction between the electronic system of the ruthenium centers and that of the pyrazine bridge.

The physical data taken together are compatible with a symmetrical structure of the two mixed-valence dimers, [II-pyz-III] and [II-bqd-III], each with two equivalent ruthenium atoms. In terms of the conventional mixed-valence language both binuclear formally Ru(II,III) ions are thus describable as delocalized or class III at least on a time scale of 10^{-8} s. In other words, if a double-well potential implying partial localization of charge is an appropriate description of [II-pyz-III] and [II-bqd-III], then it would show a central barrier of no more than 20 cm^{-1}, which is small compared to the Ru–N stretching frequencies of approximately 500 cm^{-1}.

Contribution from the Departments of Chemistry, McGill University, 801 Sherbrooke Street West, Montreal, Quebec, Canada H3A 2K6, and College Militaire Royal de St. Jean, St. Jean, Quebec, Canada G0G 1R0

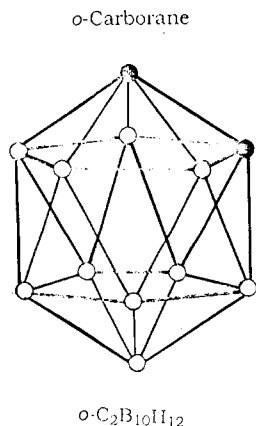# Variable-Temperature and -Pressure Vibrational Spectra of *o*-Carborane

Ralph M. Paroli,[1a] Nancy T. Kawai,[1a] Gabriel Lord,[1b] Ian S. Butler,*[,1a] and Denis F. R. Gilson*[,1a]

Variable-temperature Raman and FT-IR spectra of solid *o*-carborane have been measured. Three phases (one of which is time-dependent) were detected by Raman spectroscopy, whereas four were found by using the IR technique. Variable-pressure Raman spectra up to 70 kbar revealed a phase transition at 10.1 kbar, with pressure coefficients of 1.3 and 0.75 cm^{-1}/kbar for the in-phase, B–B stretching mode of the icosahedral cage at 773 cm^{-1} in the low- and high-pressure phases, respectively.

Introduction

The icosahedral carboranes, *o*-, *m*-, and *p*-dicarba-*closo*-do-decaborane(12) (C$_2$B$_{10}$H$_{12}$) have attracted industrial attention because of their potential use in high-temperature resistant coatings and as precursors to ceramic materials such as B$_4$C.[2] The ortho isomer, *o*-C$_2$B$_{10}$H$_{12}$, is an orientationally disordered solid at am-

o-Carborane

o-C$_2$B$_{10}$H$_{12}$

bient temperature and pressure, and its structural properties have been studied by X-ray diffraction,[3,4] differential scanning and adiabatic calorimetry,[3,5] and variable-temperature (300–11 K) IR,[6–8] Raman,[9–11] and ^{1}H and ^{11}B NMR spectroscopies.[12–14] While there is general agreement that an order–disorder phase transition exists for *o*-carborane at ~270 K, some authors have also reported other phase transitions occurring at lower temperatures, but these claims have been disputed.[10,11] It is clear,

---

(1) (a) McGill University. (b) College Militaire Royal de St. Jean.
(2) Obenland, C. O.; Papetti, S. U.S. Patent 3509216, 1970.

(3) Baughmann, R. H. *J. Chem. Phys.* **1970**, *53*, 3781.
(4) Klingen, T. J.; Kindsvater, J. H. *Mol. Cryst. Liq. Cryst.* **1974**, *26*, 365.
(5) Westrum, E. F.; Henriquez, S. H. *Mol. Cryst. Liq. Cryst.* **1976**, *32*, 31.
(6) Bartet, B.; Freymann, R.; Gandolfo, D.; Mantley, F.; Rabilloud, G.; Rossarie, J.; Sillon, B. *C. R. Seances Acad. Sci.* **1974**, *279B*, 283.
(7) Selim, M.; Capderroque, G.; Freymann, R. *C. R. Seances Acad. Sci.* **1975**, *281B*, 33.
(8) Bartet, B.; Buchs, F.; Freymann, R.; Mathey, F. *C. R. Seances Acad. Sci.* **1976**, *272B*, 531.
(9) Hones, M. J.; Shaw, D. E.; Wunderlich, F. *J. Spectrosc. Lett.* **1973**, *6*, 483.
(10) Bukalov, S. S.; Leites, L. A. *Chem. Phys. Lett.* **1982**, *87*, 327.
(11) Bukalov, S. S.; Leites, L. A. *Proc. Int. Conf. Raman Spectrosc.* **1982**, *8*, 611.
(12) Leffler, A. J.; Alexander, M. N.; Sagalyn, P. L.; Walker, N. *J. Chem. Phys.* **1975**, *63*, 3971.
(13) Beckmann, P.; Leffler, A. J. *J. Chem. Phys.* **1980**, *72*, 4600.
(14) Reynhardt, E. C.; Watton, A.; Petch, H. E. *J. Magn. Reson.* **1982**, *46*, 453.